HAL
open science

Precipitation mediates sap flux sensitivity to evaporative demand in the neotropics

Charlotte Grossiord, Bradley Christoffersen, Aura Alonso-Rodríguez, Kristina Anderson-Teixeira, Heidi Asbjornsen, Luiza Maria T. Aparecido, Z. Carter Berry, Christopher Baraloto, Damien Bonal, Isaac Borrego, et al.

▶ **To cite this version:**

HAL Id: hal-02346487
https://hal.umontpellier.fr/hal-02346487v1

Submitted on 16 Aug 2024

1   **Precipitation mediates sap flux sensitivity to evaporative demand in the neotropics**

2

3   Charlotte Grossiord[1,2]*, Bradley Christoffersen[3]*, Aura M. Alonso-Rodríguez [4], Kristina

4   Anderson-Teixeira[5,6], Heidi Asbjornsen[7], Luiza Maria T. Aparecido[8,9], Z. Carter Berry[10],

5   Christopher Baraloto[11], Damien Bonal[12], Isaac Borrego[2], Benoit Burban[13], Jeffrey Q.

6   Chambers[14,15], Danielle S. Christianson[16], Matteo Detto[17,18] , Boris Faybishenko[14], Clarissa G.

7   Fontes[19], Claire Fortunel[20,21], Bruno O. Gimenez[22], Kolby J. Jardine[15], Lara Kueppers[14],

8   Gretchen R. Miller[23], Georgianne W. Moore[9], Robinson Negron-Juarez[14], Clément Stahl[13],

9   Nathan G. Swenson[24], Volodymyr Trotsiuk[1,25,26], Charu Varadharajan[14], Jeffrey M. Warren[27],

10   Brett T. Wolfe[18,28], Liang Wei[2], Tana E. Wood[4], Chonggang Xu[2], Nate G. McDowell[29]

11

12   * These two authors contributed equally to this work.

13   [1]Swiss Federal Institute for Forest, Snow and Landscape Research WSL, Zürcherstrasse 111,

14   8903 Birmensdorf, Switzerland

15   [2]Earth and Environmental Sciences Division, Los Alamos National Laboratory, Los Alamos,

16   NM, USA

17   [3]Department of Biology and School of Earth, Environmental, and Marine Sciences, University of

18   Texas Rio Grande Valley, Edinburg, TX, USA

19   [4]USDA Forest Service, International Institute of Tropical Forestry, Jardín Botánico Sur, 1201

20   Calle Ceiba, Río Piedras, PR 00926-1115, USA

21   [5]Center for Tropical Forest Science-Forest Global Earth Observatory, Smithsonian Tropical

22   Research Institute, Panama City, Panama

23 [6]Conservation Ecology Center, Smithsonian Conservation Biology Institute, Front Royal, VA,

24 USA

25 [7]Department of Natural Resources and the Environment, University of New Hampshire, Durham,

26 NH 03824, USA

27 [8]School of Life Sciences, Arizona State University, AZ, USA

28 [9]Department of Ecosystem Science and Management, Texas A&M University, College Station,

29 TX, USA

30 [10]Schmid College of Science and Technology, Chapman University, Orange, CA, USA

31 [11]International Center for Tropical Botany (ICTB), Department of Biological Sciences, Florida

32 International University, Miami, FL, USA

33 [12]Université de Lorraine, AgroParisTech, INRA, UMR Silva, 54000 Nancy, France

34 [13]INRA, UMR EcoFoG, CNRS, Cirad, AgroParisTech, Université des Antilles, Université de

35 Guyane, 97310 Kourou, France

36 [14]Department of Geography, University of California, Berkeley, Berkeley, CA, United States

37 [15]Climate and Ecosystem Sciences Division, Lawrence Berkeley National Laboratory, Berkeley,

38 CA, United States

39 [16]Computational Research Division, Lawrence Berkeley National Laboratory, Berkeley, CA,

40 USA

41 [17]Department of Ecology and Evolutionary Biology, Princeton University, Princeton, NJ, USA

42 [18]Center for Tropical Forest Science, Smithsonian Tropical Research Institute, Panamá,

43 República de Panamá

44 [19]Department of Integrative Biology, University of California Berkeley, Berkeley, CA 94720-

45 3140, USA

46   [20]Department of Integrative Biology, University of Texas at Austin, Austin, TX, USA

47   [21]AMAP (botAnique et Modélisation de l'Architecture des Plantes et des végétations), IRD,

48   CIRAD, CNRS, INRA, Université de Montpellier, Montpellier, France

49   [22]Instituto Nacional de Pesquisas da Amazônia (INPA), Brazil

50   [23]Zachry Department of Civil Engineering, Texas A&M University, 3136 TAMU, College

51   Station, TX, USA

52   [24]Department of Biology, University of Maryland, College Park, MD, USA

53   [25]ETH Zurich, Department of Environmental Systems Science, Institute of Agricultural Sciences,

54   8092 Zurich, Switzerland

55   [26]Czech University of Life Sciences Prague, Faculty of Forestry and Wood Sciences, Kamýcká

56   129, Praha 6, Suchdol 16521, Czech Republic

57   [27]Climate Change Science Inst. and Environmental Sciences Division, Oak Ridge National

58   Laboratory, Oak Ridge, TN, USA

59   [28]School of Renewable Natural Resources, Louisiana State University, Baton Rouge, LA, USA

60   [29]Earth Systems Science Division, Pacific Northwest National Laboratory, Richland, WA, USA

61

62   **Corresponding author:** Charlotte Grossiord, charlotte.grossiord@wsl.ch, +41447392069

63

64   **Author Contributions:** CG, BC, JW and NGM planned the research. AA, HA, BB, BG, BW,

65   CB, CB, CS, CF, DB, DC, MD, BF, CF, KJ, GRM, GWM, CV, JW, BW, NS, LA, TEW and

66   LW contributed data. CG and BC analyzed the data and wrote a first draft of the manuscript, and

67   all authors contributed to revisions.

68 **Abstract**

69 Transpiration in humid tropical forests modulates the global water cycle and is a key driver of

70 climate regulation. Yet, our understanding of how tropical trees regulate sap flux in response to

71 climate variability remain elusive. With a progressively warming climate, atmospheric

72 evaporative demand (i.e., vapor pressure deficit, *VPD*) will be increasingly important for plant

73 functioning, becoming the major control of plant water use in the 21st century. Using

74 measurements in 34 tree species at seven sites across a precipitation gradient in the neotropics,

75 we determined how the maximum sap flux velocity (v_{max}) and the *VPD* threshold at which v_{max} is

76 reached (*VPD$_{max}$*) vary with precipitation regime (mean annual precipitation, *MAP*; seasonal

77 drought intensity, P_{DRY}) and two functional traits related to foliar and wood economics spectra

78 (leaf mass per area, *LMA*; wood specific gravity, *WSG*). We show that, even though v_{max} is

79 highly variable within sites, it follows a negative trend in response to increasing *MAP* and P_{DRY}

80 across sites. *LMA* and *WSG* exerted little effect on v_{max} and *VPD$_{max}$*, suggesting that these

81 widely-used functional traits provide limited explanatory power of dynamic plant responses to

82 environmental variation within hyper-diverse forests. This study demonstrates that long-term

83 precipitation plays an important role in the sap flux response of humid tropical forests to *VPD*.

84 Our findings suggest that under higher evaporative demand, trees growing in wetter

85 environments in humid tropical regions may be subjected to reduced water exchange with the

86 atmosphere relative to trees growing in drier climates.

87

88 **Keywords:** evapotranspiration, plant functional traits, transpiration, vapor pressure deficit.

4

Introduction

Humid tropical forests cover approximately 12% of global ice-free land surface area (Mayaux et al. 2005) and are characterized by high mean annual precipitation (> 1500 mm) with low variability in atmospheric temperature ($\approx 25 \pm 5°C$) (Richards 1952; Murphy and Lugo, 1986). The majority of water entering tropical forests through precipitation or rivers is returned to the atmosphere via evapotranspiration (Moreira et al. 1997; Kumagai et al. 2016). Water released by trees in their transpiration flux largely contributes to total evapotranspiration in the tropics (Schlesinger and Jasechko 2014), 35% of which is cycled back to the biome as precipitation (Eltahir and Bras 1994; Zemp et al. 2014). As such, tree transpiration in tropical forests is a major modulator of the global water cycle and plays a central role in climate regulation (Foley et al, 2007). Yet, despite our efforts in understanding transpiration patterns of tropical trees (e.g., Meinzer et al. 2003; Stahl et al. 2013a; Maréchaux et al. 2018), how trees regulate water use in these ecosystems remains one of the largest uncertainty components in models of tropical evapotranspiration.

At daily to seasonal time-scales, trees regulate their transpiration flux in response to variation in atmospheric evaporative demand (i.e., vapor pressure deficit, *VPD*), radiation, wind and available soil water (Oren et al. 1999; Meinzer et al. 2001). Under non-limiting soil water availability, radiation and *VPD* are usually the most significant climate variables controlling water flux in tropical trees (e.g., Meinzer et al. 2008). However, global warming will result in an exponential climb in *VPD* in the next decades (Zhang et al. 2015), and the relative role of these two abiotic drivers (i.e., radiation *vs*. *VPD*) is expected to shift in the future with *VPD* becoming the major control of plant water use in the 21st century (Novick et al. 2016). Therefore, improving our understanding of water use patterns and their response to *VPD*, including the

112   linkages to predictive plant traits, is an important next step with major implications for global

113   climate and vegetation predictions.

114   While over long periods (i.e. years to decades), stand water use is mainly regulated by

115   changes in leaf area and species composition, over short-term periods (i.e. hours to days), trees

116   regulate sap flux velocity (v) (Edwards et al. 1996) through changes in stomatal conductance.

117   Thus, v response to daily VPD variation directly depends on the degree of stomatal closure

118   (Schulze et al. 1972). Under low VPD conditions, plant stomata are fully open and v increases

119   linearly with VPD (Franks et al. 1997), until v reaches a saturation rate (v_{max}, Fig. 1) at a given

120   VPD threshold (VPD_{max}, Fig. 1). As VPD increases, trees progressively start closing their

121   stomata, and for some species, including tropical trees, stomatal closure can be so pronounced as

122   to result in a decreased rate of v (Fig. 1) (Schulze et al. 1972; Franks et al. 1997). The degree of

123   sap flux response to VPD varies both within and between species because of differences in local

124   climatic adjustments and ecological strategy. For instance, trees originating from distinct

125   precipitation regimes should differ in their sap flux responses to VPD because of adaptive

126   mechanisms in response to moisture conditions, including wood hydraulic properties and foliar

127   traits (Mencuccini 2003; Poyatos et al. 2007). Trees growing in drier climates may produce

128   xylem elements with reduced lumen areas relative to trees from wetter climates to reduce the risk

129   of xylem embolism and promote overall hydraulic safety (Hacke et al. 2004; Fonti and Jansen

130   2012). Anatomical changes in these conductive tissues will directly alter the sap flux patterns of

131   trees (i.e. reduced v in drier systems), and have been associated to reduced VPD_{max} and v_{max} in

132   dry ecosystems (Grossiord et al. 2017; 2018). Similarly, reductions in soil moisture during dry

133   periods have been linked with changes in stomatal density (Luomala et al. 2005) and in the

134   synthesis of chemical signals inducing stomatal closure (Schachtman and Goodger 2008), which

135   should also reduce VPD_{max} and v_{max} in forests that are subjected to seasonal droughts. In humid

136   tropical forests, regional variability in annual precipitation (from 1500 to > 4000 mm annually)

137   and in dry season intensity is high, suggesting large variation in plant physiological and

138   structural adjustments to moisture status, and thus potentially important differences in VPD_{max}

139   and v_{max} between ecosystems. However, soil moisture is usually less limiting in humid tropical

140   forests than in temperate and semiarid regions where reductions in VPD_{max} and v_{max} following

141   precipitation reduction have been reported (Grossiord et al. 2018). As such, this characteristic

142   physiological or hydraulic adjustment to soil moisture limitation may not occur in this biome,

143   suggesting that acclimation processes to water stress would only occur under a given

144   precipitation and/or drought intensity threshold.

145   A difficulty in making predictions on the functioning of humid tropical forests lies in the

146   fact that these ecosystems host more tree species than any other terrestrial ecosystem (Myers et

147   al. 2000). Large species diversity in the tropics is accompanied by large diversity in plant

148   functional traits (Wright et al. 2007; Baraloto et al. 2010; Fortunel et al. 2012; 2014; Zhu et al.

149   2013; Cosme et al. 2017). Functional differences that directly alter v regulation include rooting

150   properties (e.g. water uptake depth, Stahl et al. 2013b; Brum et al. 2019), hydraulic properties

151   (e.g. lumen area or water potential at 50% loss of hydraulic conductivity P_{50}; Litvak et al. 2012)

152   and foliar characteristics (e.g. stomatal density or leaf turgor loss point; Bartlett et al. 2012,

153   Maréchaux et al. 2018). However, while such mechanistic trait data are growing in availability

154   for tropical forests, they remain poorly quantified relative to more easily measurable traits such

155   as leaf mass per area (*LMA*) and wood specific gravity (*WSG*) (Wright et al. 2004; Chave et al.

156   2014). *LMA* and *WSG* respectively comprise the well-studied leaf and wood economics spectra,

157   which have been successfully related to various aspects of plant function along a fast (resource-

158   acquisitive, low *LMA* and *WSG*)-to-slow (resource-conservative, high *LMA* and *WSG*) continuum

159   (Reich et al. 1997; but see Baraloto et al. 2010; Fortunel et al. 2012). These traits only indirectly

160   relate to dynamic physiological processes such as F_D (Brodribb 2017), however *LMA* and *WSG*

161   can be used to support mechanistic theory of moisture adjustments in modelling frameworks by

162   correlating with other plant traits related to hydraulic transport (Christoffersen et al. 2016). As

163   such, we might expect trees originating from drier regions in humid tropical forests, and thus

164   with lower VPD_{max} and v_{max}, to have higher *LMA* and *WSG* (i.e. two typical adjustment responses

165   to reduced moisture, Wright et al. 2005) relative to trees with higher VPD_{max} and v_{max}.

166   Here we analyzed how trees regulate sap flux velocity in response to *VPD* variation in 34

167   species originating from seven sites along a precipitation gradient in the neotropics. Our

168   objectives were to test how long-term local precipitation regime (annual precipitation and

169   intensity of the dry season) modulate VPD_{max} and v_{max}, and detect whether variation in VPD_{max}

170   and v_{max} across sites can be related to the variability in two easy-to-measure functional traits:

171   *LMA* and *WSG*. We hypothesized that:

172   1) trees growing in relatively dry regions and that are subjected to more frequent and intense

173   droughts would show reduced VPD_{max} and v_{max} compared to trees originating from wetter

174   areas because of long-term physiological and structural adjustments to reduced soil

175   moisture availability (Mencuccini 2003) (Fig. 1),

176   2) across all sites, trees with higher *LMA* and *WSG* would show reduced VPD_{max} and v_{max}

177   relative to trees with low *LMA* and *WSG*.

8

Material and methods

Study sites

178

179

180   We used data collected from mature humid tropical forests in seven sites spanning from

181 Puerto Rico to northern Brazil (Table 1, Figs. S1 & S2). The focal sites are located in Puerto

182 Rico (SAB hereafter), Costa Rica (SOL), Panama (SLZ, BCI and PNM), French Guiana (FRG)

183 and Brazil (MAN). The target tree species pool (representing among the most abundant tree

184 species within each site) varied between four and nine per site (Table 2), leading to a total of 34

185 tree species included in this study with only one species being present at multiple sites (Table

186 S1). Climatic conditions (rainfall, air temperature, atmospheric humidity and solar radiation)

187 were measured continuously and recorded by local weather stations at all sites during the

188 measurements.

189   All sites, apart from the SOL site, experience a dry season (i.e., monthly precipitation <

190 100 mm) of approx. three months. Long-term precipitation was used to characterize long-term

191 annual moisture status and drought intensity in each site using the site-level average in annual

192 sum of precipitation (MAP) and monthly precipitation during the dry season (P_{DRY}) over the

193 1950-2010 period. When long-term site-specific data was not available (all sites except PNM,

194 BCI and SLZ), long-term precipitation was extracted for each site using Twentieth Century

195 Reanalysis Project, a 2.0-degree latitude and 2.0-degree longitude global climate dataset (Compo

196 et al. 2011). The sites were characterized by contrasting precipitation regimes varying between

197 1826 and 4200 mm on average annually over the 1950-2010 period, with the PNM site (Panama)

198 being the driest and the SOL site (Costa Rica) the wettest (PNM < MAN < BCI < SLZ < FRG <

199 SAB < SOL) (Table 1). See Table 1 for more details on site characteristics and site-specific

200 references.

201

Sap flux measurements

203   In each site between four and nine trees that occupied dominant positions in the canopy (to

204   avoid effects related to crown exposure) were selected for this study, leading to a total of 43 trees

205   (Table 2). At all sites, tree sap flux velocity (v; cm h^{-1}) was measured every 10 min, 15 min, 30

206   min or hour using either the thermal dissipation method (Granier 1987) or the heat ratio method

207   (Burgess et al. 1998). Depending on the site, sensors were bought from manufacturers (SFM1,

208   ICT International, NSW, Australia; UP-Gmbh, Cottbus, Germany; PS-GP, PlantSensors, Nakara,

209   Australia) or lab-built. Measurements were conducted continuously for periods varying between

210   two and 24 months (Table 1) between January 2014 and January 2017. For the thermal

211   dissipation method, sensors (i.e. one sensor per tree except for the SOL site where two sensors

212   per tree were installed, 10- or 20-mm long) were installed in the sapwood at 1.3 m aboveground

213   or above buttresses with a 10 cm vertical spacing between probes. For the heat-ratio method (i.e.

214   one sensor per tree), each set of sensors consisted of two or three thermocouples and one-line

215   heater probe. The thermocouples were inserted at 1.3 m aboveground at depths varying between

216   2.2 and 3 cm below the cambium. The sensors were covered with reflective insulation to reduce

217   the risk of direct sunlight causing thermal gradients. The data were recorded continuously by

218   dataloggers (CR800, CR10X and CR1000, Campbell Scientific Corp., Logan, UT, USA), apart

219   from the SFM1 sensors that contain a stand-alone datalogger. For more details see the site-

220   specific references in Table 1.

221

Sap flux data processing

223   Each site's sap flux data files were accompanied by a standardized metadata reporting

224   framework, consisting of three associated metadata files, respectively describing the data files,

225   the columns of each data file, and field observations of tree size, canopy position, and species

226   identity, if available (Christianson et al. 2017). We collated the raw data for all sites via a series

227   of R scripts, which interpreted each dataset in terms of its associated metadata file (code

228   available in the supplement of Christianson et al. 2017).

229   We started data processing using the raw mV values outputted by the sap flux sensors.

230   Sap flux velocity data from the SOL site had already been converted to v (cm h^{-1}) using the

231   Granier equation (1987) (see Aparecido et al. 2016 for more details). The open-source *Baseliner*

232   software (Oishi et al. 2016) was used to calculate v values for each tree following the equation

233   proposed by Granier (1987). No species-specific equations are available for the tropical species

234   included in this study, and thus care must be taken when interpreting v results as the empirically

235   derived coefficients in the Granier equation may introduce errors in v calculations (Bush et al.

236   2010). *Baseliner* enables users to control the quality and process data using a combination of

237   automated steps and manual editing (Oishi et al. 2016). Missing data were gap filled when they

238   were shorter than two hours using linear interpolation (Oishi et al. 2016). Estimation of baseline

239   nighttime flow is done automatically in *Baseliner* based on a joint set of conditions, including

240   nighttime hours (characterized by near-zero radiation), stable temperature differential between

241   probes (estimated using coefficient of variation) and low *VPD* (see Oishi et al. 2016 for more

242   details).

243   After converting all values into v, we conducted a systematic removal of values

244   associated with measurement failures and sensor removals in the field. For the MAN, PNM, SLZ

245   and BCI sites, we removed all days before DOY 175 in 2016 (corresponding to the 2015-2016

11

246   ENSO event) to avoid potential v responses to anomalously low soil moisture (Fig. S3). In

247   addition, sub-hourly v data was visually assessed for all trees to ensure no drought period was

248   included in the final dataset. The FRG site included semi-deciduous tree species, which

249   experienced leaf drop during the measurement periods. To avoid effects related to changes in

250   leaf area induced by significant leaf drop, these periods were removed from the analyses.

251   Individual-tree v time series are presented for each site in Fig. S4. The two methods used for

252   measuring v (heat ratio method vs. thermal dissipation method) have been shown to vary in their

253   accuracy to measure absolute v rates (Steppe et al. 2010). However, tests conducted at the MAN

254   and SLZ sites (i.e. the two sites where the heat ratio method was used), where both sensor types

255   were collocated on individual trees, indicated no significant differences in v rates between the

256   two methods (Fig. S5). No information on the depth of the active sapwood was available for the

257   target trees, but to our knowledge, no study reported radial changes in v patterns to VPD

258   variation.

259

260   *Estimation of maximum sap flux velocity and VPD at which sap flux velocity reaches maximum*

261   *values*

262   To avoid confounding effects of radiation we applied a radiation filter for each site by

263   removing all v data where sub-hourly radiation was below the 90th percentile of daytime

264   radiation values. For most sites this threshold was equal to 600 W m^{-2} apart for the BCI and FRG

265   sites where the threshold was equal to 700 W m^{-2} (Fig S6). Using sub-hourly v data, we estimated

266   the maximum sap flux velocity (v_{max}, Fig. 1) for each tree as the 95th percentile of v values after

267   applying the radiation filter (Fig. S7). The VPD value at which v reaches maximum levels

268   ($VPD_{max,}$ Fig. 1) was estimated as the 2.5[th] percentile of VPD values corresponding to v_{max} (Fig.

269   S7). All the analysis was done using the R language for statistical computing (3.2.1, R

270   Development Core Team 2015).

271

272   *Functional traits*

273   To analyze how variation in VPD_{max} and v_{max} could be related to foliar and wood

274   functional traits, we used leaf mass per area (*LMA,* g m^{-2}) and wood specific gravity (*WSG,* g cm^{-}

275   ^{3}). Investigation of other traits (e.g., wood anatomy, leaf-to-sapwood area ratio) revealed a

276   paucity of data for the target tree species, thus we focused strictly on *LMA* and *WSG*. When

277   possible, we used direct measurements on the sampled trees during the sap flux measurements.

278   Conversely, when the trait measurements were not available for our focal trees, we used

279   previously published data originating from the same species (see sources in Table S1). In total,

280   data on *LMA* and *WSG* were gathered for 31 (73%) and 39 (91%) trees (for *LMA* and *WSG*,

281   respectively) (Table S1).

282

283   *Statistical analyses*

284   The impacts of long-term *MAP* (or P_{DRY}), *LMA* and *WSG* on VPD_{max} and v_{max} were

285   determined first by fitting linear models, followed by closer examination using linear mixed

286   effect models (package *lme*) where *MAP* (or P_{DRY}), *LMA*, *WSG*, diameter at breast height (*DBH*,

287   i.e. to account for effects related to tree size) and their interactions were used as fixed effects,

288   and trees nested in sites was used as a random effect. The model selection procedure started with

289   all variables and by progressively removing the variables with the lowest explanatory power

290   until the minimal model with the lowest Akaike Information Criterion (AIC) was obtained.

291   Models were compared using 'anova' test to select the least complex parsimonious model. In all

292   cases, the linear model (package *lm*) with *MAP* or P_{DRY} was selected. The same tests were used

293   to detect the impact of *MAP* (or P_{DRY}) on *LMA* and *WSG*, with *MAP* (or P_{DRY}), *DBH* and their

294   interaction used as fixed effects.

295 **Results**

296 *Climatic conditions*

297   Precipitation during the measurements was similar to the long-term average precipitation

298 (1950-2010) in all sites (Fig. S3). Mean daily air temperature and *VPD* ranged from 18 to 28°C,

299 and 0.47 to 2.94 kPa, respectively, during the measurement period, depending on the sites and

300 seasons (Fig. S8). The sites experienced a range of *VPD* values during sap flux measurements

301 varying between 0 and approx. 4.3 kPa (Fig. 2).

302

303 *Sap flux response to VPD variation*

304   Strong variability in sap flux velocity (v) was observed within sites, reflecting the

305 important diversity of water use strategies between species (Fig. S4). For most trees, v increased

306 linearly with *VPD* until reaching a saturation rate (v_{max}) at a given *VPD* threshold (VPD_{max}, Fig.

307 2). For a few trees, v decreased with rising *VPD* after reaching a saturation rate, suggesting

308 strong stomatal closure, while other trees showed no distinctive saturation rate with rising *VPD*

309 (Fig. 2). Trees displaying a decline in v at high *VPD* did not have significantly different *LMA* or

310 *WSG* from trees without such a decline (Welch's two-sided t-test: t = 0.257, df = 4.05, P = 0.810;

311 t = 0.169, df = 4.75, P = 0.873, respectively). In general, v_{max} was reached when VPD_{max} varied

312 between 0.6 and 2.0 kPa, depending on the trees (Fig. 2). v_{max} varied between 4.1 and 41.4 cm h^{-1}

313 ^{1}, depending on the individual tree (Fig. 2).

314   VPD_{max} and v_{max} were highly variable across sites, with a tendency for lower mean values

315 at wetter sites and higher values at drier sites. The driest site, PNM, had the highest values (mean

316 of 1.5 kPa and 24.7 cm h^{-1} for VPD_{max} and v_{max}, respectively), while the wettest site, SOL, had

317   the lowest v_{max} (mean of 7.7 cm h^{-1}). There were significant negative effects of *MAP* on v_{max} (r^2 =

318   0.32, slope = -0.006, *P* < 0.001) but not on VPD_{max} (r^2 = 0.10, slope = -0.000, *P* = 0.062) (Fig. 3).

319   A significant negative effect of P_{DRY} was found for v_{max} (r^2 = 0.21, slope = -0.21, *P* = 0.005), but

320   not for VPD_{max} (r^2 = 0.00, slope = -0.000, *P* = 0.842) (Fig. 3). No relationship was found between

321   VPD_{max} and v_{max} (Fig. S9), indicating no trade-off between the *VPD* threshold at which *v* levels-

322   off at maximum rates and maximum *v*.

323

324   *Relationships with functional traits*

325   No effect of *LMA* on v_{max} (r^2 = 0.00, *P* = 0.835), and VPD_{max} (r^2 = 0.00, *P* = 0.704) was

326   found. Similarly, no relationship between *WSG* and v_{max} (r^2 = 0.08, *P* = 0.167), and VPD_{max} (r^2 =

327   0.02, *P* = 0.542) were found (Fig. 4). There was no effect of *MAP* or P_{DRY} on *LMA* (*P* = 0.722

328   and *P* = 0.600, respectively), nor on *WSG* (*P* = 0.434 and *P* = 0.290). A significant relationship

329   was observed between *LMA* and *WSG* (Fig. S9), suggesting a slight coupling between leaf and

330   stem economics in these trees (i.e. trees with higher *LMA* tend to grow denser wood).

Discussion

Precipitation mediates sap flux response to evaporative demand in the neotropics

Our findings highlight that sap flux response to VPD under non-depleted soil moisture conditions in humid tropical forests partially depends on average MAP and P_{DRY} over the last 50 years, i.e., indicators of long-term moisture availability and drought stress intensity. More specifically, our data show that as average site-level precipitation increases and seasonal drought intensity decreases, trees attain lower maximum sap flux (v_{max}) when soil moisture is non-limiting (Fig. 3). This relationship was not an artefact of reduced radiation at wetter sites because of the radiation filter applied (Fig. S6). These findings contrast with previous observations from Mediterranean and semiarid woodlands where increasing aridity resulted in reduced v_{max} (e.g., Poyatos et al. 2007; Grossiord et al. 2018), suggesting contrasting underlying adjustments to moisture between supply-limited and demand-limited environments.

The negative response pattern of v_{max} to increasing MAP and P_{DRY} observed here implies that compared to dry temperate forests, tree sap flux velocity in humid tropical forests does not depend on drought-adjustments to local climate (i.e. adjustments reducing the vulnerability to water shortage) (Grossiord et al. 2018). Instead, sap flux patterns in response to climate variability are probably dependent on adjustments to high-moisture conditions. Indeed, in the sites included here, VPD is usually low and precipitation is high compared to temperate and semiarid regions, thus tree water relations are more rarely limited by high evaporative demand or drought stress. One may therefore expect trees in this environment to have evolved functional traits to deal with other limiting factors such as low radiation induced by the high cloud cover (Moore et al. 2018). Furthermore, high atmospheric humidity can lead to sustained leaf wetness with water films on leaves inhibiting gas exchanges, and resulting in reduced sensitivity to

17

354   atmospheric drivers (Dawson and Goldsmith 2018; Moore et al. 2018). Plants that grow in high

355   atmospheric humidity conditions have also been reported to show low levels of endogenous

356   abscisic acid (ABA) (Nejad and Van Meeteren 2007; Okamoto et al. 2009), and marginal

357   stomata regulation on carbon and water fluxes (Torre and Fjeld 2001; Torre et al. 2003).

358   Therefore, an important research topic for future work, in addition to exploring adjustment

359   mechanisms to reduced precipitation, is to understand how adaptive mechanisms related to high

360   moisture could relate to sap flux regulation in tropical trees.

361   Lower v_{max} under non-limiting soil moisture conditions could potentially result in reduced

362   water exchange with the atmosphere in humid tropical forests as more days with high VPD are

363   likely to occur in the future. Currently, Earth system models (ESM) are being developed to

364   incorporate plant hydraulic traits (Xu et al. 2016, Christoffersen et al. 2016, Kennedy et al.

365   2019), but it is not immediately clear if such traits will produce the patterns observed here for

366   humid tropical ecosystems. Incorporating traits related to adjustments to high-moisture

367   environments could potentially affect the differential responses of global precipitation to

368   vegetation changes (e.g., Kooperman et al. 2018). To gain further insight into the drivers of sap

369   flux variability, we suggest extending this work to more extreme sites, i.e. both wet and dry, and

370   exploring other relevant factors such as long-term indices of evaporative demand (Poyatos et al.

371   2007). Improved quantification of within-site variation, including systematic replication of

372   species sampled along environmental gradients would also be needed. Such an improved design

373   would be valuable for trait-enabled dynamic vegetation models (Fisher et al. 2018), even if

374   systematically sampling the same species in tropical forests may prove complicated considering

375   their high species diversity.

376

Common functional traits provide limited insights into the mechanisms of sap flux regulation in the neotropics

We found a large variability in *LMA* and *WSG* within and across sites, reflecting the high functional diversity present in these ecosystems (Fortunel et al. 2012). Nevertheless, the large diversity in these functional traits could not be related to the variability in VPD_{max} and v_{max} observed across sites (Fig. 4). This is not so surprising in light of a recent review (Moles 2018) that highlights a remarkable degree of inconsistency in reported relationships of *LMA* and *WSG* with other plant traits related to plant ecological strategy or the fast-slow economic spectrum (Reich 2014). Moreover, we expect that stem and leaf traits more directly related to acquisition, transport, and retention of water (hydraulic traits) would underpin the patterns observed here; appropriate trait selection is therefore critical for uncovering trait-moisture relationships more generally (Griffin-Nolan et al. 2018). Specifically, reduction in moisture across large environmental gradients has been associated with shifts in mechanistic foliar traits such as stomatal density (e.g. Luomala et al. 2005) or chemical compounds inducing stomatal closure (Schachtman and Goodger 2008). Investigating such anatomical and chemical foliar adjustments that provide stronger mechanistic basis than *LMA* will be needed to unravel the underlying adaptive processes driving VPD_{max} and v_{max} patterns along our precipitation gradient (Fig. 3). Similarly, *WSG* had no detectable impact on VPD_{max} and v_{max} (Fig. 4). Wood density is considered an important modulator of xylem water transport as higher wood density has been associated with reduced hydraulic conductivity and higher resistance to xylem cavitation (Hacke et al. 2004). As such, this property could constrain the maximum flux of water movement in trees (Barbour and Whitehead 2003). However, most *WSG* measurements, including the ones used in this study, are made using main stems. Yet, to be relevant for water transport, this trait

19

400   should represent all woody tissues, from the roots to the canopy (Fortunel et al. 2012).

401   Furthermore, the interpretation of *WSG* as an indicator of plant hydraulic functions is debated

402   (Larjavaara and Muller-Landau 2010), since a given *WSG* can be achieved under various

403   combinations of wood anatomy which do not necessarily impact water transport, but instead

404   reflect variability in the competing demands of strength and storage (Fortunel et al. 2014;

405   Zieminska et al. 2015; Morris et al. 2016; Dias et al. 2019).

406   Therefore, although *LMA* and *WSG* are useful for indicating, respectively, placement on

407   the leaf economics spectrum (Wright et al. 2004) and successional status in productivity models

408   (Moorcroft et al. 2001), they do so only at global scales and do not consistently relate to other

409   plant traits at local and regional scales (Moles 2018), as our findings also confirm here. They

410   appear to provide limited interpretation of dynamic plant responses to environmental variation

411   within hyper-diverse tropical forests (Brodribb 2017). While incorporation of such local

412   adjustments in ESMs is possible via trait-mediated plant responses to the environment (e.g.,

413   Fisher et al. 2015), the functional traits explored here, *LMA* and *WSG*, show little promise.

414   Focused data collection on more mechanistic traits associated with plant hydraulics and stomatal

415   function like for instance P_{50}, leaf turgor loss point, cuticular conductance, sapwood anatomy,

416   stomatal density or foliar chemical compounds are likely to reveal mechanistic controls on the

417   interspecific differences in sap flow observed here, which can be used to refine existing plant

418   hydraulic models (Christoffersen et al. 2016; Wolf et al. 2016; Xu et al. 2016; Sperry et al.

419   2017).

420

421   *Conclusion*

422   This study demonstrates that local climate plays an important role in the sap flux

423   response of humid tropical forests to evaporative demand. Moreover, we highlight that trees

424   growing in wetter regions in the tropics may be subjected to a reduced sap flux velocity with the

425   high evaporative demand predicted by most climate models. We expect incorporating these

426   regulation strategies in models could improve our prediction accuracy of both vegetation

427   dynamics and water cycles. This study also shows that easy-to-measure functional traits provide

428   little interpretation in dynamic sap flux response to *VPD*, suggesting that more mechanistic traits

429   should be investigated to build predictors in future models. Finally, it is important to note that

430   although our sampling included a large number of species relative to previous studies

431   investigating sap flux-climate responses, our work still covers only a limited range of the

432   incredible diversity present in humid tropical forests. Extending sap flux measurements in more

433   regions in the tropics and developing large databases of plant water use (e.g. SAPFLUXNET,

434   Poyatos et al. 2016) is an important next step if we want to improve our predictive capacity of

435   tropical forest responses to climate change.

450   **References**

451   Aparecido LMT, Miller GR, Cahill AT, Moore GW (2016) Comparison of tree transpiration

452   under wet and dry canopy conditions in a Costa Rican premontane tropical forest. Hydrological

453   Processes 30, 26: 5000-5011.

454   Baraloto C, Timothy Paine CE, Poorter L, Beauchene J, Bonal D, Domenach A-M, Hérault B,

455   Patiño S, Roggy J-C, Chave J (2010) Decoupled leaf and stem economics in rain forest trees.

456   Ecology Letters 13: 1338-1347.

457   Barbour MM, Whitehead D (2003) A demonstration of the theoretical prediction that sap

458   velocity is related to wood density in the conifer Dacrydium cupressinum. New Phytologist 158:

459   477–488.

460   Bartlett MK, Scoffoni C, Sack L (2012) The determinants of leaf turgor loss point and prediction

461   of drought tolerance of species and biomes: a global meta‐analysis. Ecology Letters 15: 393-405.

462   Bonal D, Bosc A, Ponton S, Goret J-Y, Burban B, Gross P, Bonnefond J-M, Elbers J, Longdoz

463   B, Epron D, Guehl J-M, Granier A (2008) Impact of severe dry season on net ecosystem

464   exchange in the Neotropical rainforest of French Guiana. Global Change Biology 14: 1917-1933.

465   Brodribb TJ (2017) Progressing from 'functional' to mechanistic traits. New Phytologist 215: 9-

466   11.

467   Brum M, Vadeboncoeur MA, Ivanov V, Asbjornsen H, Saleska S, Alves LF, Penha D, Dias JD,

468   Aragão LE, Barros F, Bittencourt P (2019) Hydrological niche segregation defines forest

469   structure and drought tolerance strategies in a seasonal Amazon forest. Journal of Ecology,

470   https://doi.org/10.1111/1365-2745.13022

471   Burgess SS, Adams MA, Turner NC, Ong CK (1998) The redistribution of soil water by tree root

472   systems. Oecologia 115: 306-311.

473   Burgess SS, Adams MA, Turner NC, Beverly CR, Ong CK, Khan AA, Bleby TM (2001) An

474   improved heat pulse method to measure low and reverse rates of sap flow in woody plants. Tree

475   Physiology 21: 589-598.

476   Bush SE, Hultine KR, Sperry JS, Ehleringer JR (2010) Calibration of thermal dissipation sap

477   flow probes for ring-and diffuse-porous trees. Tree Physiology 30: 1545-1554.

478   Cate RB, Nelson LA (1971) A simple statistical procedure for partitioning soil test correlation

479   data into two classes. Soil Science Society of America Proceedings 35: 658-660.

480   Chave J, Rejou-Mechain M, Burquez A, Chidumay E, Colgan MS, Delitti WBC et al. (2014)

481   Improved allometric models to estimate the aboveground biomass of tropical trees. Global

482   Change Biology 20: 3177–3190.

483   Christianson DS, Varadharajan C, Christofferson B, Detto M, Faybishenko BA, Jardine KJ,

484   Negron-Juarez R, Gimenez BO, Pastorello GZ, Powell T, Warren J, Wolfe B, Chambers JC,

485   Kueppers LM, McDowell NG, Agarwal D (2017) A metadata reporting framework for

486   standardization and synthesis of ecohydrological field observations for ecosystem model

487   parameterization and benchmarking. Ecological Informatics 42: 148-58.

488   Christoffersen BO et al. (2016) Linking hydraulic traits to tropical forest function in a size-

489   structured and trait-driven model (TFS v. 1-Hydro). Geoscientific Model Development 9: 4227.

490   Compo GP et al. (2011) The Twentieth Century Reanalysis Project. Quarterly Journal of the

491   Royal Meteorological Society 137: 1-28.

492   Cosme LHM, Schietti J, Costa FRC, Oliveira RS (2017) The importance of hydraulic

493   architecture to the distribution patterns of trees in a central Amazonian forest. New Phytologist

494   215: 113-125.

495   Dawson TE, Goldsmith GR (2018) The value of wet leaves. New Phytologist 219: 1156-1169.

496   Detto M, Wright SJ, Calderón O, Muller-Landau HC (2018). Resource acquisition and

497   reproductive strategies of tropical forest in response to the El Niño–Southern Oscillation. Nature

498   communications 9: 913.

499   Dias AS, Oliveira RS, Martins FR, Bongers F, Anten NPR, Sterck F (2019) How do lianas and

500   trees change their vascular strategy in seasonal versus rain forest? Perspectives in Plant Ecology,

501   Evolution and Systematics 40: 125465.

502   Edwards WRN, Becker P, Èermák J (1997). A unified nomenclature for sap flow measurements.

503   Tree Physiology 17: 65-67.

504   Eltahir EAB, Bras RL (1994). Precipitation recycling in the Amazon basin. Quarterly Journal of

505   the Royal Meteorological Society 120: 861-880.

506   Fauset S, Baker TR, Lewis SL, Feldpausch TR, Affum-Baffoe K, Foli EG, Hamer KC, Swaine

507   MD, Etienne R (2012) Drought-induced shifts in the floristic and functional composition of

508   tropical forests in Ghana. Ecology Letters 15: 1120-1129.

509   Fisher RA et al. (2015) Taking off the training wheels: the properties of a dynamic vegetation

510   model without climate envelopes, CLM4. 5 (ED). Geoscientific Model Development 3593-3619.

511   Fisher RA et al. (2018) Vegetation demographics in Earth System Models: A review of progress

512   and priorities. Global Change Biology 24: 35-54.

513   Foley JA et al. (2007) Amazonia revealed: forest degradation and loss of ecosystem goods and

514   services in the Amazon Basin. Frontiers in Ecology and the Environment 5: 25-32.

515   Fonti P, Jansen S (2012) Xylem plasticity in response to climate. New Phytologist 195: 734-736.

516   Fortunel C, Fine PVA, Baraloto C, Dalling J (2012) Leaf, stem and root tissue strategies across

517   758 Neotropical tree species. Functional Ecology 26: 1153-1161.

518   Fortunel C, Ruelle J, Beauchene J, Fine PV, Baraloto C (2014) Wood specific gravity and

519   anatomy of branches and roots in 113 Amazonian rainforest tree species across environmental

520   gradients. New Phytologist 202: 79-94.

521   Franks PJ, Cowan IR, Farquhar GD (1997) The apparent feedforward response of stomata to air

522   vapour pressure deficit: information revealed by different experimental procedures with two

523   rainforest trees. Plant, Cell & Environment 20: 142-145.

524   Good SP, Moore GW, Miralles DG (2017) A mesic maximum in biological water use

525   demarcates biome sensitivity to aridity shifts. Nature Ecology & Evolution 1: 1883.

526   Gleason SM, Butler DW, Zieminska K, Waryszak P, Westoby M (2012) Stem xylem

527   conductivity is key to plant water balance across Australian angiosperm species. Functional

528   Ecology 26: 343–352.

529   Granier A (1987) Evaluation of transpiration in a Douglas-fir stand by means of sap flow

530   measurements. Tree Physiology 3: 309-320.

531   Griffin-Nolan RJ, Bushey JA, Carroll CJW, Challis A, Chieppa J, Garbowski M, Hoffmann AM,

532   Post AK, Slette IJ, Spitzer D, Zambonini D (2018) Trait selection and community weighting are

533   key to understanding ecosystem responses to changing precipitation regimes. Functional Ecology

534   32: 1746-1756.

535 Grossiord C, Sevanto S, Borrego I, Chan AM, Collins AD, Dickman LT, Hudson P, McBranch

536 N, Michaletz ST, Pockman WT, Vilagrosa A, McDowell NG (2017) Tree water dynamics in a

537 drying and warming world. Plant, cell & environment 40: 1861-1873

538 Grossiord C, Sevanto S, Limousin JM, Meir P, Mencuccini M, Pangle RE, Pockman WT,

539 Salmon Y, Zweifel R, McDowell NG (2018) Manipulative experiments demonstrate how long-

540 term soil moisture changes alter controls of plant water use. Environmental and Experimental

541 Botany 152: 19-27

542 Hacke UG, Sperry JS, Pittermann J (2004) Analysis of circular bordered pit function II.

543 Gymnosperm tracheids with torus-margo pit membranes. American Journal of Botany 91: 386-

544 400.

545 Hogg EH, Hurdle PA (1997) Sap flow in trembling aspen: implications for stomatal responses to

546 vapor pressure deficit. Tree Physiology 17: 501-509.

547 Kennedy D, Swenson S, Oleson KW, Lawrence DM, Fisher R, Lola da Costa AC, Gentine P

548 (2019) Implementing plant hydraulics in the Community Land Model, version 5. Journal of

549 Advances in Modeling Earth Systems 11: 485-513.

550 Kimball BA, Alonso-Rodríguez AM, Cavaleri MA, Reed SC, González G, Wood TE. (2018)

551 Infrared heater system for warming tropical forest understory plants and soils. Ecology &

552 Evolution, 8, 1932–1944.

553 Kooperman GJ et al. (2018) Forest response to rising CO_2 drives zonally asymmetric rainfall

554 change over tropical land. Nature Climate Change 8 : 434.

555 Koenker R (2017) Quantreg: quantile regression. R package version 5.33. R Foundation for

556 Statistical Computing, Vienna.

557 Kumagai T, Kanamori H, Chappell NA (2016) Tropical forest hydrology. Forest Hydrology:

558 Processes, Management and Assessment 88-102.

559 Lange OL, Lösch R, Schulze ED, Kappen L (1971) Responses of stomata to changes in

560 humidity. Planta 100: 76-86.

561 Larjavaara M, Muller-Landau HC (2010) Rethinking the value of high wood density. Functional

562 Ecology 24: 701-705.

563 Limousin JM et al. (2012) Morphological and phenological shoot plasticity in a Mediterranean

564 evergreen oak facing long-term increased drought. Oecologia 169: 565-577.

565 Litvak E, McCarthy HR, Pataki DE (2012) Transpiration sensitivity of urban trees in a semi-arid

566 climate is constrained by xylem vulnerability to cavitation. Tree physiology 32: 373-388.

567 Luomala E, Laitinen K, Sutinen S, Kellomäki S, Vapaavuori E (2005) Stomatal density, anatomy

568 and nutrient concentrations of Scots pine needles are affected by elevated CO_2 and temperature.

569 Plant, Cell & Environment 28: 733-749.

570 Luizão RC, Luizão FJ, Paiva RQ, Monteiro TF, Sousa LS, Kruijt B (2004) Variation of carbon

571 and nitrogen cycling processes along a topographic gradient in a central Amazonian forest.

572 Global Change Biology 10: 592-600.

573 Malhi Y, Wright J (2004) Spatial patterns and recent trends in the climate of tropical rainforest

574 regions. Philosophical Transactions of the Royal Society B: Biological Sciences 359: 311-329.

575 Malhi Y (2009) Exploring the likelihood and mechanism of a climate-change-induced dieback of

576 the Amazon rainforest. Proceedings of the National Academy of Sciences 106: 20610.

577 Mangiafico S (2018) rcompanion: Functions to Support Extension Education Program

578 Evaluation. R package version 2.0.0. https://CRAN.R-project.org/package=rcompanion

579   Maréchaux I, Bonal D, Bartlett MK, Burban B, Coste S, Courtois EA, Dulormne M, Goret J-Y,

580   Mira E, Mirabel A, Sack L, Stahl C, Chave J (2018) Dry-season decline in tree sapflux is

581   correlated with leaf turgor loss point in a tropical rainforest. Functional Ecology, doi:

582   10.1111/1365-2435.13188.

583   Martinez-Cabrera HI, Jones CS, Espino S, Schenk HJ (2009) Wood anatomy and wood density

584   in shrubs: responses to varying aridity along transcontinental transects. American Journal of

585   Botany 96: 1388–1398.

586   Mayaux P, Holmgren P, Achard F, Eva H, Stibig HJ, Branthomme A (2005) Tropical forest

587   cover change in the 1990s and options for future monitoring. Philosophical Transactions of the

588   Royal Society B: Biological Sciences 360: 373-384.

589   Meinzer FC, Goldstein G, Andrade JL (2001) Regulation of water flux through tropical forest

590   canopy trees: do universal rules apply? Tree Physiology 21: 19-26.

591   Meinzer FC, James SA, Goldstein G, Woodruff D (2003) Whole-tree water transport scales with

592   sapwood capacitance in tropical forest canopy trees. Plant, Cell & Environment 26: 1147–1155.

593   Meinzer FC, Woodruff DR, Dome, J-C, Goldstein G, Campanello PI, Gatti MG, Villalobos-

594   Vega R (2008) Coordination of leaf and stem water transport properties in tropical forest trees.

595   Oecologia 156: 31–41.

596   Mencuccini M (2003) The ecological significance of long- distance water transport: short- term

597   regulation, long- term acclimation and the hydraulic costs of stature across plant life forms.

598   Plant, Cell & Environment 26: 163-182.

599   Moles AT (2018) Being John Harper: Using evolutionary ideas to improve understanding of

600   global patterns in plant traits. Journal of Ecology 106:1-18.

601 Monteith JL (1995) A reinterpretation of stomatal responses to humidity. Plant, Cell &

602 Environment 18: 357-364.

603 Moorcroft PR, Hurtt GC, Pacala SW (2001) A method for scaling vegetation dynamics: the

604 ecosystem demography model (ED). Ecological monographs 71: 557-586.

605 Moore GW, Orozco G, Aparecido LM, Miller GR (2018) Upscaling transpiration in diverse

606 forests: Insights from a tropical premontane site. Ecohydrology 11: e1920.

607 Moreira M *et* al. (1997) Contribution of transpiration to forest ambient vapor based on isotopic

608 measurements. Global Change Biology 3: 439-450.

609 Morris H, Plavcová L, Cvecko P, Fichtler E, Gillingham MA, Martínez-Cabrera HI, McGlinn

610 HI, Wheeler DJ, Zheng E, Ziemińska K, Jansen S (2016) A global analysis of parenchyma tissue

611 fractions in secondary xylem of seed plants. New Phytologist 209: 1553-1565.

612 Murphy PG, Lugo AE (1986) Ecology of tropical dry forest. Annual review of ecology and

613 systematics 17: 67-88.

614 Myers N, Mittermeier RA, Mittermeier CG, Da Fonseca GA, Kent J (2000) Biodiversity

615 hotspots for conservation priorities. Nature 403: 853.

616 Nejad AR, Van Meeteren U (2007) The role of abscisic acid in disturbed stomatal response

617 characteristics of Tradescantia virginiana during growth at high relative air humidity. Journal of

618 Experimental Botany 58: 627–636.

619 Novick KA et al. (2016). The increasing importance of atmospheric demand for ecosystem water

620 and carbon fluxes. Nature Climate Change 6: 1023.

621 Oishi AC, Hawthorne DA, Oren R (2016) Baseliner: an open-source, interactive tool for

622 processing sap flux data from thermal dissipation probes. SoftwareX 5: 139-143.

623   Okamoto M, Tanaka Y, Abrams SR, Kamiya Y, Seki M, Nambara E (2009) High humidity

624   induces abscisic acid 8 '‐ hydroxylase in stomata and vasculature to regulate local and systemic

625   abscisic acid responses in arabidopsis. Plant Physiology 149L: 825–834.

626   Oren R, Sperry JS, Katul GG, Pataki DE, Ewers BE, Phillips N, Schäfer KVR (1999) Survey and

627   synthesis of intra‐and interspecific variation in stomatal sensitivity to vapour pressure deficit.

628   Plant, Cell & Environment 22 : 1515-1526.

629   Poyatos R, Martínez-Vilalta J, Čermák J, Ceulemans R. Granier A, Irvine J, Köstner B,

630   Lagergren F, Meiresonne L, Nadezhdina N, Zimmermann R, Llorens P, Mencuccini M (2007)

631   Plasticity in hydraulic architecture of Scots pine across Eurasia. Oecologia 153 : 245–259.

632   Poyatos R, Granda V, Molowny-Horas R, Mencuccini M, Steppe K, Martínez-Vilalta J (2016)

633   SAPFLUXNET: towards a global database of sap flow measurements. Tree Physiology 36:

634   1449-1455.

635   R Core Team (2015) R: A language and environment for statistical computing. R Foundation for

636   Statistical Computing, Vienna, Austria. URL http://www.R-project.org/.

637   Reich PB, Walters MB, Ellsworth DS (1997) From tropics to tundra: global convergence in plant

638   functioning. Proc Natl Acad Sci USA 94: 13730–13734

639   Reich PB (2014) The world-wide 'fast–slow'plant economics spectrum: a traits manifesto.

640   Journal of Ecology 102: 275-301.

641   Richards PW (1952) The tropical rain forest; an ecological study. At The University Press;

642   Cambridge.

643   Schachtman DP, Goodger JQ (2008) Chemical root to shoot signaling under drought. Trends in

644   plant science 13: 281-287.

645 Schlesinger WH, Jasechko S (2014) Transpiration in the global water cycle. Agricultural and

646 Forest Meteorology 189: 115-117.

647 Schulze E-D, Lange OL, Buschbom U, Kappen L, Evenari M (1972) Stomatal responses to

648 changes in humidity in plants growing in the desert. Planta 108: 259–270.

649 Slot M, Winter K (2017) In situ temperature response of photosynthesis of 42 tree and liana

650 species in the canopy of two Panamanian lowland tropical forests with contrasting rainfall

651 regimes. New Phytologist 214: 1103-1117.

652 Stahl C, Burban B, Wagner F, Goret JY, Bompy F, Bonal D (2013a) Influence of Seasonal

653 Variations in Soil Water Availability on Gas Exchange of Tropical Canopy Trees. Biotropica 45:

654 155-164.

655 Stahl C, Hérault B, Rossi V, Burban B, Bréchet C, Bonal D (2013b) Depth of soil water uptake

656 by tropical rainforest trees during dry periods: does tree dimension matter? Oecologia 173: 1191-

657 1201.

658 Steppe K, De Pauw DJ, Doody TM, Teskey RO (2010) A comparison of sap flux density using

659 thermal dissipation, heat pulse velocity and heat field deformation methods. Agricultural and

660 Forest Meteorology 150: 1046-1056.

661 Swenson NG et al. (2017) Tree co-occurrence and transcriptomic response to drought. Nature

662 communications 8: 1996.

663 Togashi HF et al. (2015) Morphological and moisture availability controls of the leaf area- to-

664 sapwood area ratio: analysis of measurements on Australian trees. Ecology & Evolution 5: 1263-

665 1270.

666   Torre S, Fjeld T (2001) Water loss and postharvest characteristics of cut roses grown at high or

667   moderate relative air humidity. Scientia Horticulturae 89: 217–226.

668   Torre S, Fjeld T, Gislerød HR, Moe R (2003) Leaf anatomy and stomatal morphology of

669   greenhouse roses grown at moderate or high air humidity. Journal of the American Society for

670   Horticultural Science 128: 598–602.

671   van der Sande MT et al. (2016) Old-growth Neotropical forests are shifting in species and trait

672   composition. Ecological Monographs 86: 228-243.

673   Whitehead D, Okali DUU, Fasehun FE (1981) Stomatalresponse to environmental variables in

674   two tropical forestspecies during the dry season in Nigeria. Journal of Applied Ecology 18: 571–

675   587.

676   Wolf A, Anderegg WR, Pacala SW (2016) Optimal stomatal behavior with competition for water

677   and risk of hydraulic impairment. Proceedings of the National Academy of Sciences 113: E7222-

678   E7230.

679   Wood PJ, Hannah DM, Sadler JP (Eds.) (2008) Hydroecology and ecohydrology: past, present

680   and future. John Wiley & Sons.

681   Wright IJ et al. (2004) The worldwide leaf economics spectrum. Nature 428: 821–827.

682   Wright IJ et al. (2005) Modulation of leaf economic traits and trait relationships byclimate. Glob.

683   Ecol. Biogeogr. 14: 411–421.

684   Wright IJ et al. (2007) Relationships Among Ecologically Important Dimensions of Plant Trait

685   Variation in Seven Neotropical Forests. Annals of Botany 99: 1003-1015.

686 Xu X, Medvigy D, Powers JS, Becknell JM, Guan K (2016) Diversity in plant hydraulic traits

687 explains seasonal and inter-annual variations of vegetation dynamics in seasonally dry tropical

688 forests. New Phytologist 212: 80-95.

689 Zemp DC, Schleussner CF, Barbosa HMJ, Van der Ent RJ, Donges JF, Heinke J, Sampaio G,

690 Rammig A (2014) On the importance of cascading moisture recycling in South America.

691 Atmospheric Chemistry and Physics 14: 13337-13359.

692 Zhang K, Kimball JS, Nemani RR, Running SW, Hong Y, Gourley JJ, Yu Z (2015) Vegetation

693 greening and climate change promote multidecadal rises of global land evapotranspiration. Sci.

694 Rep. 5: doi:10.1038/srep15956.

695 Zhu SD, Song JJ, Li RH, Ye Q (2013) Plant hydraulics and photosynthesis of 34 woody species

696 from different successional stages of subtropical forests. Plant Cell Environ 36: 879-891.

697 Ziemińska K, Westoby M, Wright IJ (2015) Broad Anatomical Variation within a Narrow Wood

698 Density Range—A Study of Twig Wood across 69 Australian Angiosperms. PLoS ONE 10:

699 e0124892.

700 **Table 1:** Characteristics of the study sites

Site code	PNM	MAN	BCI	FRG	SLZ	SAB	SOL
Country	Panama	Brazil	Panama	French Guiana	Panama	Puerto Rico	Costa Rica
MAT* (°C), MAP* (mm)	26, 1826	27, 2200	26, 2640	26, 3102	25, 3286	24, 3500	24, 4200
P_{DRY}* (mm)	53	95	60	72	70	90	100
Topography	Light slope	Flat	Flat	Light slope	Steep	Light slope	Steep
Soil depth (m)	> 6	> 20	NA	> 15	> 3	> 20	1.5
Elevation (m)	30	100	170	40	130	130	540
Mean LAI* ($m^2 m^{-2}$)	NA	6.0	6	6.7	NA	6.47	3.32
Soil type	Mollisol	Latosol	Oxisol	Acrisols	Oxisol	Ultisol	Andisol
MET station (m)*	25	50	48	56	52	2	42
Sap flux method	TD	HR	TD	TD	HR	TD*	TD
Duration of the measurements (months)	12	2-5	16	24	13	12	21
References	Slot & Winter, 2017	Luizão et al., 2004	Detto et al., 2018	Bonal et al., 2008	Slot & Winter, 2017	Kimball et al., 2018	Aparecido et al., 2016

701 *MAP*, mean annual sum of precipitation (1950-2010); *MAT*, mean annual temperature (1950-2010); *P_{DRY}, mean monthly sum of precipitation*
702 *during the dry season; LAI*, leaf area index; HR, heat-ratio method; TD, thermal dissipation method; *MET station*, height of the meteorological
703 station (m).

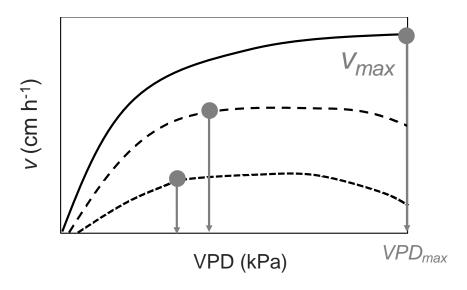704 **Table 2:** Characteristics of the study trees (± SE).

Site	Number of measured trees	Mean tree height (m)	Mean *DBH** (cm)	Number of target species
PNM	4	30.7 ± 2.7	83.9 ± 18.9	4
MAN	4	32.2 ± 1.5	59.9 ± 9.6	4
BCI	6	26.6 ± 2.0	47.3 ± 6.7	5
FRG	5	27.8 ± 2.1	40.3 ± 10.9	5
SLZ	6	28.1 ± 1.5	49.9 ± 4.5	6
SAB	9	23.4 ± 0.9	28.8 ± 1.8	8
SOL	8	30.1 ± 1.1	96.7 ± 24.5	4

705
706
707
708
709
710
711
712
713
714

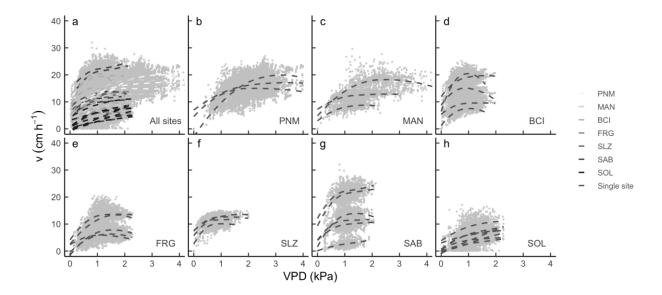715 *DBH* = diameter at breast height

Figure legends

717 **Figure 1:** Theoretical variation in sap flux velocity (v) response to VPD: under low VPD

718 conditions, v increases linearly with rising VPD until v reaches a saturation rate (v_{max}, grey circle)

719 at a given VPD threshold (VPD_{max}, grey arrow). As VPD progressively increases v will either

720 level-off at a maximum rate or start dropping progressively. Differences in v responses to

721 increasing VPD between trees (highlighted by different dotted and bold lines) emerge from long-

722 term adjustments to local moisture conditions (i.e. reflecting differences in foliar and wood

723 hydraulic properties), with reductions in moisture expected to result in lower VPD_{max} and v_{max}.

724 **Figure 2:** Sub-hourly sap flux velocity (v, cm h^{-1}) as a function of vapor pressure deficit (VPD,

725 kPa) for each site. Sites are organized going from the driest (b) to the wettest (h) (i.e. in terms of

726 *MAP*). Dashed lines represent fitted curves using local regression function for each individual

727 tree.

728 **Figure 3:** Relationships between the VPD threshold at which sap flux levels-off at maximum

729 levels ($VPD_{max} \pm$ SD, kPa) and maximum sap flux ($v_{max} \pm$ SD, cm h^{-1}), and mean annual

730 precipitation (*MAP*, mm) (panels a and c) or monthly precipitation during the dry season (P_{DRY},

731 mm) (panels b and d). Asterisks, situated next to the r^2 values, denote the significance of the

732 relationships (* $P < 0.05$, ** $P < 0.01$, *** $P < 0.001$).

733 **Figure 4:** Relationships between VPD threshold at which sap flux levels-off at maximum levels

734 (VPD_{max}, kPa) and maximum sap flux (v_{max}, cm h^{-1}), and wood specific gravity (WSG, g cm^{-3})

735 (panels a and c) or leaf mass per area (LMA, g m^{-2}) (panels b and c), across all sites. Each point

736 represents a different individual tree.

737

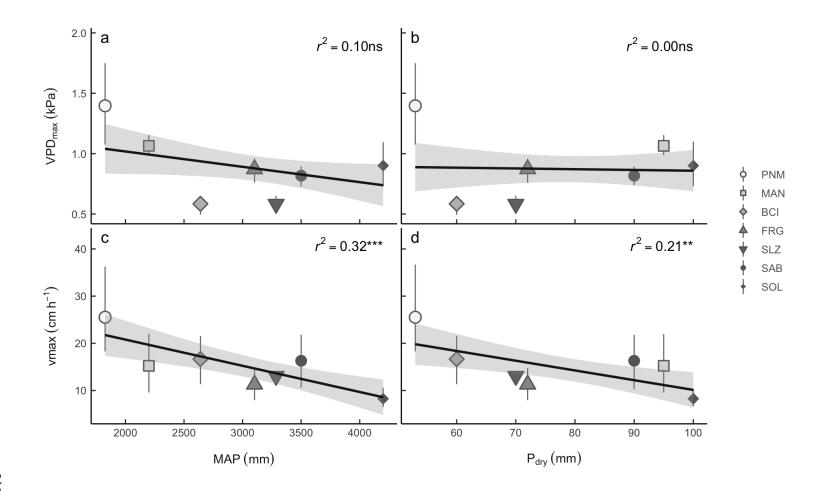738   **Figure 1**

739
740
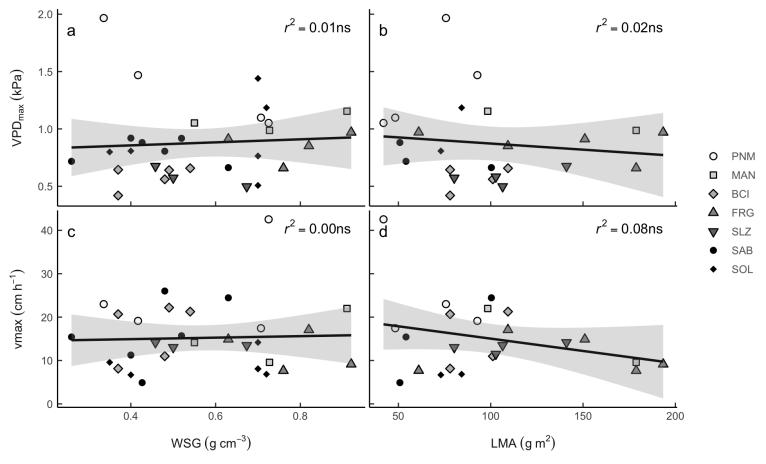
Figure 2

Figure 3

Figure 4